Characterizing native and hydrocarbon-stapled enfuvirtide conformations with ion mobility mass spectrometry and hydrogen–deuterium exchange

Stocks, Bradley B.; Bird, Gregory H.; Walensky, Loren D.; Melanson, Jeremy E.

Publisher's version / Version de l'éditeur:
https://doi.org/10.1021/jasms.0c00453
Journal of the American Society for Mass Spectrometry, 32, 2, pp. 753-761, 2021-02-03

Characterizing Native and Hydrocarbon-stapled Enfuvirtide Conformations with Ion Mobility Mass Spectrometry and Hydrogen/Deuterium Exchange

Bradley B. Stocks[a]*, Gregory H. Bird[b], Loren D. Walensky[b], and Jeremy E. Melanson[a]

[a]*National Research Council Canada, Metrology*

1200 Montreal Road, Ottawa, Ontario, Canada K1A 0R6

[b]*Dana-Farber Cancer Institute*

450 Brookline Avenue, Boston, Massachusetts, USA 02215

*Corresponding author

bradley.stocks@nrc-cnrc.gc.ca
Tel: 613-993-4416
ORCID: 0000-0002-7265-9344

ABSTRACT

The number of approved peptide therapeutics, as well as those in development, has been increasing in recent years. Frequently, the biological activity of such peptides is elicited through adoption of secondary structural elements upon interaction with their cellular target. Many therapeutic peptides however are unstructured in solution and accordingly exhibit poor bioavailability due to rapid proteolysis *in vivo*. To combat this degradation, numerous naturally-occurring peptides with therapeutic properties contain stabilizing features such as N-to-C cyclization or disulfide bonds. Recently hydrocarbon stapling, via non-native amino acid substitution followed by ring-closing metathesis, has been shown to induce dramatic stabilization of α-helical peptides. Identifying the ideal staple location along the peptide backbone is a critical developmental step and methods to streamline this optimization are needed. Mass spectrometry-based methods such as ion mobility (IM) and hydrogen-deuterium exchange (HDX) can detect multiple discrete peptide conformations, a significant advantage over bulk spectroscopic techniques. In this study we use IM-MS and HDX-MS to demonstrate that the native 36-residue enfuvirtide peptide is highly dynamic in solution, and that the conformational ensemble populated by stabilized constructs depends heavily upon staple location. Further, our measurements yield results that correlate well with the averaged α-helical content measured by circular dichroism. The MS-based approaches described herein represent sensitive and potentially high-throughput methods for characterizing and identifying optimally stapled peptides.

INTRODUCTION

Peptide therapeutics have historically received less attention than small molecule drugs and protein therapeutics, such as antibodies. This discrepancy stems from inherent disadvantages of peptides, including biological instability (short half-life) and limited membrane permeability.[1] However, multiple strategies to increase the bioavailability and efficacy of peptide drugs have recently emerged, and accordingly the number of approved peptide therapeutics has been steadily increasing.[2-5] Examples of such stabilizing approaches include conjugation with small molecules,[6] polymers,[7] or glycans,[8] incorporating protease resistant non-natural or D-amino acids,[6, 9] and constraining the structural flexibility through electrostatic interaction optimization.[10]

An alternative approach to peptide structural stabilization is hydrocarbon stapling,[11-13] which is applied to peptides adopting an α-helical active conformation. Stapled peptides can inhibit protein-protein interactions,[14] and have demonstrated utility in treating cancer and disrupting inflammatory pathways[15] and viral fusion.[16] During peptide synthesis, non-native amino acid residues are introduced into the sequence and their olefin-containing side chains are linked via ring-closing metathesis.[17] The amino acid positions within the peptide are chosen so as to maintain the bioactive interaction surface with the resulting staple spanning one or two helical turns. Induction of α-helical content by introduction of a staple correlates with an increase in target affinity and proteolytic stability, however, the degree of stabilization can be strongly dependent on the staple type and location.[18, 19]

Due to the helical dependence on staple location, a suite of stabilized peptide constructs is often produced during development. Methods that can assess the resulting conformations in a medium-to-high throughput manner could efficiently reduce the number of potential leads selected for further investigation. The utility of mass spectrometry (MS) methods to structurally characterize proteins is well-demonstrated,[20-22] and two such techniques – hydrogen/deuterium exchange (HDX) MS[23-25] and ion mobility (IM) MS[26] – are used frequently in the pharmaceutical industry.

Accordingly, HDX-MS results are included in regulatory filings for new protein drugs and IM-MS data is likely to be appended in the future.[27] In addition to protein studies, HDX-MS is used to interrogate peptide conformational dynamics both in solution[28] and the gas phase,[29] while IM-MS facilitates gas-phase detection of changes to peptide conformational ensembles in response to various stimuli, such as ligand binding[30], proline isomerization,[31, 32] or disulfide-bond scrambling.[33] Conformational dynamics measured by HDX-MS have been shown to correlate with proteolytic stability for a series of stabilized borealin peptides differing only in their staple positions.[28] Further, comparative conformational analyses of GLP-1 and variants stabilized by hydrocarbon-stitching revealed that HDX-MS was more effective than circular dichroism at identifying differences in structural stabilization. In vitro proteolysis testing was the most sensitive method for detecting the differential impact of staple variants on structural stability and, most profoundly, the stability profile was predictive of in vivo activity.[34] However, to our knowledge IM-MS has yet to be leveraged in stapled peptide assessments.

Enfuvirtide (Enf) is a 36-residue fusion inhibitor peptide that was approved by the FDA in 2003 for the treatment of HIV-1.[35, 36] The Enf sequence is derived from the heptad repeat 2 and membrane-proximal external region domains of the viral gp41 protein, and adopts an α-helical conformation that interrupts six-helix bundle formation.[37] However, experimental studies demonstrate that Enf exhibits only marginal and transient helicity in solution,[18, 38] and these findings are supported by molecular dynamics (MD) simulations, regardless of whether a disordered or helical starting structure is employed.[39] Interestingly, a 42-residue Enf construct including flanking resides from the gp41 sequence shows partial helicity in the C-terminal half of the sequence by NMR and MD.[38-40] Recently it has been demonstrated that stabilized Enf constructs can differ widely in their α-helical character as a function of staple location[18] – a common observation in stapled-peptide studies.[19, 28]

In this work, we utilize IM-MS and HDX-MS to assess the conformation and dynamics of native Enf as well as various hydrocarbon-stapled derivatives. The chosen location for a

hydrocarbon staple can dramatically affect the helical induction and therapeutic efficacy of the resultant peptide.[41] Our data reveal that the conformations populated in the gas-phase, as well as the conformational dynamics in solution, depend heavily on where the staple is located in the sequence. We demonstrate that, for the Enf constructs studied here, IM readouts as well as early timepoint HDX-MS data correlate well with average α-helicity measured by circular dichroism. Overall our results suggest that multiple MS datasets could be used in an initial screen of staple locations to identify optimally-structured constructs for advancement to biological testing.

MATERIALS AND METHODS

Peptide Preparation

All peptides used in this study were synthesized, purified, quantified, analyzed by circular dichroism (CD), and subjected to in vitro proteolysis testing as previously described.[11] Peptides were produced on an Apex 396 (Aapptec) automated peptide synthesizer using Rink amide AM LL resin (EMD Biosciences, 0.2 mmol/g resin), at 50 μmol scale. The standard Fmoc protocol employed 2 × 10 min deprotections in 20% piperidine/NMP followed by a pair of consecutive methanol and dimethylformamide washes. The incorporated nonnatural amino acids were treated with 4 × 10 min incubations in 20% piperidine/NMP to achieve complete deprotection. Amino acid coupling was performed using 0.4 M stock solutions of Fmoc-protected amino acids, 0.67 M 2-(6-chloro-1H-benzotriazole-1-yl)-1,1,3,3-tetramethylaminium hexafluorophosphate, and 2 M N,N-diisopropyl ethylamine, yielding 1 mL of 0.2 M active ester (4 equivalents). Coupling frequency and incubation times were 2 × 30 min for standard residues, 2 × 45 min for the olefinic nonnatural amino acids, and 3 × 45 min for the residue following a nonnatural amino acid. For CD spectra,

peptides were dissolved in 5 mM potassium phosphate (pH 7.5) to a final concentration of 50 μM and percent helicity was calculated based on the theoretical maximum for a 36-residue peptide.[11]

Ion Mobility Mass Spectrometry

Peptides were serially diluted from DMSO stocks into 10 mM ammonium acetate (Sigma, St. Louis, MO), pH 6.7, to 5 μM and infused at 5 μL min^{-1} into the electrospray source of a Waters Synapt G2 (Milford, MA) Q-TOF mass spectrometer operating in positive ionization mode. Ion source and transmission parameters were minimized to avoid gas-phase conformational activation, as described previously.[42] Briefly, the electrospray needle was held at 2 kV and the cone voltage was set to 20 V. The source and desolvation temperatures were 25 °C and 40 °C, respectively. Traveling wave ion mobility (TWIM) separation was achieved in N_2 with a wave velocity of 800 m s^{-1} and a 40 V wave height. Arrival time distributions were converted to collision cross sections (CCS) via calibration of the TWIM separation using a 10 mM polyalanine (Sigma) solution in 49.5:49.5:1 water:methanol:acetic acid and published CCS values determined in nitrogen gas.[43] Ion mobility data were analyzed using MassLynx 4.1 (Waters) and average CCS values were calculated as previously described.[44] Gaussian peak fitting was performed in OriginPro 2016 (OriginLab, Northampton, MA) and CCS distribution widths were determined at 5% base peak intensity. The CCS value for the isolated Enf helix from crystal structure 2x7r[45] (chain C, residues 638-673) was calculated via the trajectory method using Collidoscope.[46]

Hydrogen/Deuterium Exchange Mass Spectrometry

Enfuvirtide peptide solutions in DMSO were diluted with 10 mM sodium phosphate buffer pH 7.0, resulting in a stock concentration of 25 μM. Isotope exchange was initiated by 14-fold dilution into D_2O (Cambridge Isotope Laboratories, Andover, MA) exchange buffer (10 mM sodium

phosphate in 90 % D_2O, pD 7.0) at room temperature. The final DMSO concentration was ~0.3 % (v/v). At various time points ranging from 10 s to 4 h, aliquots were removed and the exchange quenched via a 1:1 dilution into 150 mM sodium phosphate pH 2.5 at 0 °C, followed by rapid freezing in liquid nitrogen. Undeuterated controls were prepared in an identical manner, except that all buffers were formulated in H_2O. For LC-MS analysis, samples were gently thawed and injected onto a Waters BEH130 C8 (2.1 x 50 mm) column via a Rheodyne 7725 injector. Chromatography was carried out with a Thermo Fisher Scientific Vanquish UHPLC (San Jose, CA) using a water:acetonitrile gradient in the presence of 0.1 % formic acid. The solvent lines, injector, and column were immersed in ice to allow separation to proceed at 0 °C. Column eluent was directed into the HESI source of an Orbitrap Fusion Lumos (Thermo Fisher Scientific) mass spectrometer. Data were acquired in positive ionization mode with a needle voltage of 3.5 kV and ion transfer tube and desolvation temperatures of 300 °C and 250 °C, respectively. All mass spectra were exported from Xcalibur software and the 3+ and 4+ charge states of each peptide were used for deuterium uptake analysis in HXExpress.[47, 48] No correction for back-exchange was performed therefore deuterium uptake values are reported as relative.[49]

RESULTS AND DISCUSSION

Investigation into the Enf conformational ensemble was enabled with the use of multiple structurally-constrained constructs. The sequences investigated (Table 1) contain a single *i, i+4* hydrocarbon staple,[11] localized to the N-terminal (SAH-gp41$_{(638\text{-}673)}$(C)), central (SAH-gp41$_{(638\text{-}673)}$(B)), or C-terminal region (SAH-gp41$_{(638\text{-}673)}$(D), SAH-gp41$_{(638\text{-}673)}$(E)). All subsequent solution- and gas-phase experiments were conducted on native Enf and the four stapled peptides. To aid in data interpretation, additional ion mobility experiments were performed on select double-stapled Enf constructs (*details in Supporting Information*).

ENF	YTSLIHSLIEESQNQQEKNEQELLELDKWASLWNWF
SAH-gp41$_{(638\text{-}673)}$(B)	YTSLIHSLIEESQNQ**X**EKN**X**QELLELDKWASLWNWF
SAH-gp41$_{(638\text{-}673)}$(C)	YT**X**LIH**X**LIEESQNQQEKNEQELLELDKWASLWNWF
SAH-gp41$_{(638\text{-}673)}$(D)	YTSLIHSLIEESQNQQEKNEQELLEL**X**KWA**X**LWNWF
SAH-gp41$_{(638\text{-}673)}$(E)	YTSLIHSLIEESQNQQEKNEQELLELDK**X**ASL**X**NWF

Table 1. Amino acid sequences of enfuvirtide constructs. Red "X" corresponds to the non-native amino acid substituted to enable hydrocarbon stapling and red bars indicate the staple positions.

Enf Secondary Structure Monitored by Circular Dichroism

Enfuvirtide must adopt an α-helical structure to carry out its inhibitory activity against HIV fusion,[50] however CD spectroscopy revealed that native Enf is largely disordered in solution (Fig. S1), in accordance with previous studies.[10, 18, 38, 40, 50] A minor amount of α-helicity is nonetheless observed—19% when compared to a fully-helical theoretical peptide of equal length.[11] For all Enf constructs assessed here, hydrocarbon-stapling resulted in an increase in helicity, as measured at 222 nm, and followed the trend of native < SAH-gp41$_{(638\text{-}673)}$(C) < SAH-gp41$_{(638\text{-}673)}$(E) < SAH-gp41$_{(638\text{-}673)}$(B) << SAH-gp41$_{(638\text{-}673)}$(D). The dramatic difference in helical content between SAH-gp41$_{(638\text{-}673)}$(E) and SAH-gp41$_{(638\text{-}673)}$(D), despite only a two amino acid frameshift in the staple location is notable, and a similar helical dependence on staple location has been measured for an unrelated viral peptide.[16] While many biomolecules can populate multiple conformations in solution, CD reports only on the global average. Therefore, in an attempt to further define the Enf structural ensemble, we employed mass spectrometry-based techniques capable of detecting co-existing conformations.

Multiple Native Enf Conformations Observed by IM-MS

We used traveling-wave IM-MS to first investigate the native Enf conformational ensemble. The mass spectrum displayed a narrow charge state distribution dominated by the $[M+4H]^{4+}$ ion (Fig. S2), similar to previous reports.[51] The more highly charged ions (5+, 6+)

exhibited only a single conformer due to charge repulsion (Fig. 1a), while low charge states (3+, 4+) presented multiple conformations. The dominant $[M+4H]^{4+}$ ion gave rise to a deconvoluted CCS distribution consisting of four species (Fig. 1b) and will be the focus of all subsequent comparisons. Peptide or protein conformational heterogeneity is manifested in the width of the cross section distribution[52, 53] and the greater than 150 $Å^2$ width for the Enf $[M+4H]^{4+}$ ion suggest several contributing peptide structures. Multiple studies have demonstrated that helical conformers exhibit larger cross sections than disordered peptides.[54-58] It is thus reasonable to hypothesize that the Enf conformer at 1078 $Å^2$ results from a mostly helical species, while the remainder of the distribution consists of an ensemble of partially helical and disordered structures. This observation is supported by recent molecular dynamics simulations showing that Enf maintains no ordered structure in solution, but rather exists in a rapid equilibrium between a partially helical structure and globular conformations made up mostly of beta turns.[39, 59] Further, using the Collidoscope software package,[46] the calculated CCS for the 4+ charge state of a fully helical Enf peptide[45] was 1153 $Å^2$, only ~7 % larger than our experimental measurement of the largest Enf conformer.

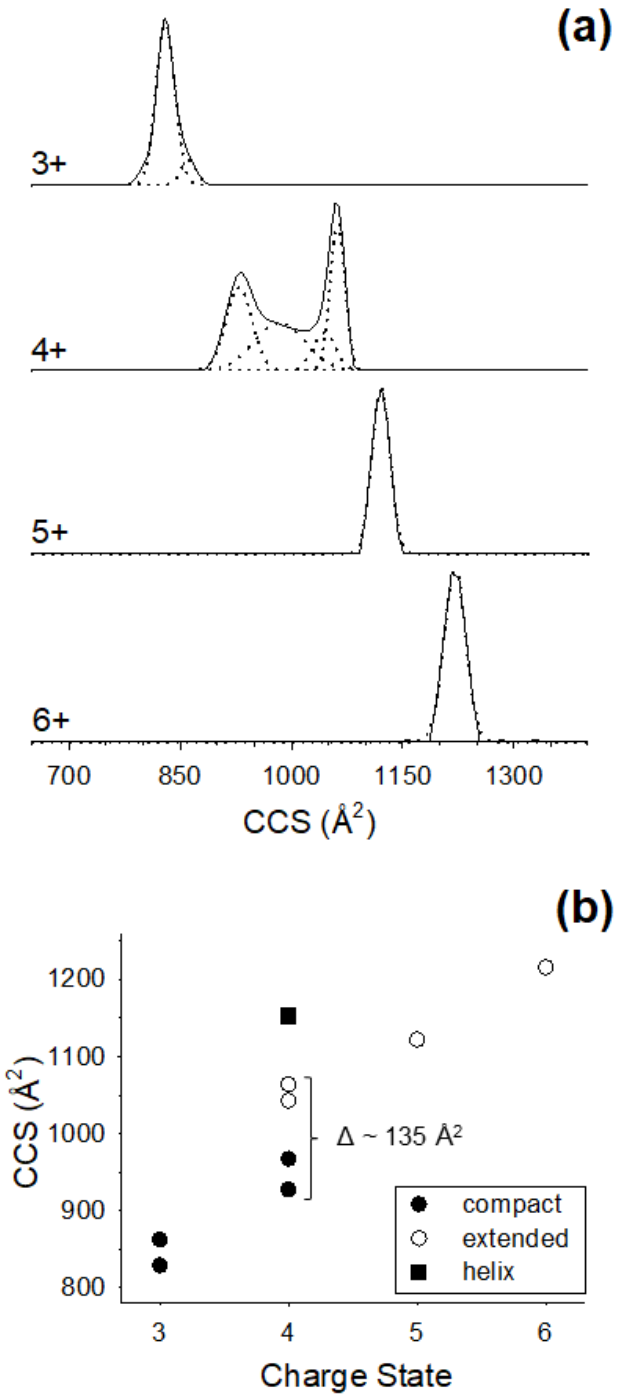

Figure 1. (a) Native enfuvirtide collision cross section distributions for charge states 3+ to 6+. (b) Enf peak maxima from Gaussian fits as a function of charge state. Filled and open circles correspond to compact and extended species, respectively. In all cases, the standard deviation of triplicate measurements are <1 % and the corresponding error bars are smaller than the data point symbols. The filled square represents the calculated CCS for a fully helical Enf peptide (details in text).

Gas-Phase Enf Ensembles Depend on Hydrocarbon Staple Location

In an effort to delineate the multiple conformers observed in the native Enf CCS distribution, we acquired IM-MS data for the four singly-stapled constructs listed in Table 1, and Figure 2 shows the resultant CCS distributions for the $[M+4H]^{4+}$ charge states. The SAH-gp41$_{(638-673)}$(C) construct exhibits a CCS trace (Fig. 2b) nearly identical in shape to native Enf, albeit shifted to a slightly higher CCS. The SAH-gp41$_{(638-673)}$(E) construct (Fig. 2c) also presents multiple conformers, separated by 115 Å^2, however the ensemble is much more discretely segregated into two populations. While both the SAH-gp41$_{(638-673)}$(C) and SAH-gp41$_{(638-673)}$(E) constructs display multiple conformers by IM, they exhibit only slightly more helicity than native Enf (Fig. S1). The centrally-stapled construct, SAH-gp41$_{(638-673)}$(B), is approximately twice as helical as native Enf (Fig. S1), and the CCS distribution is considerably skewed toward the more extended conformer (Fig. 2d). A small proportion of more condensed conformations is still present, however they are almost completely absent in SAH-gp41$_{(638-673)}$(D) (Fig. 2e). The CCS distribution measured for the SAH-gp41$_{(638-673)}$(D) construct consists of a single, relatively narrow peak that aligns quite well with the extended conformer observed in native Enf. SAH-gp41$_{(638-673)}$(D) also exhibits the most helicity by CD—2.5-fold greater than that of native Enf—and thus the extended species around 1075 Å^2 is hypothesized to result from a helical conformer.

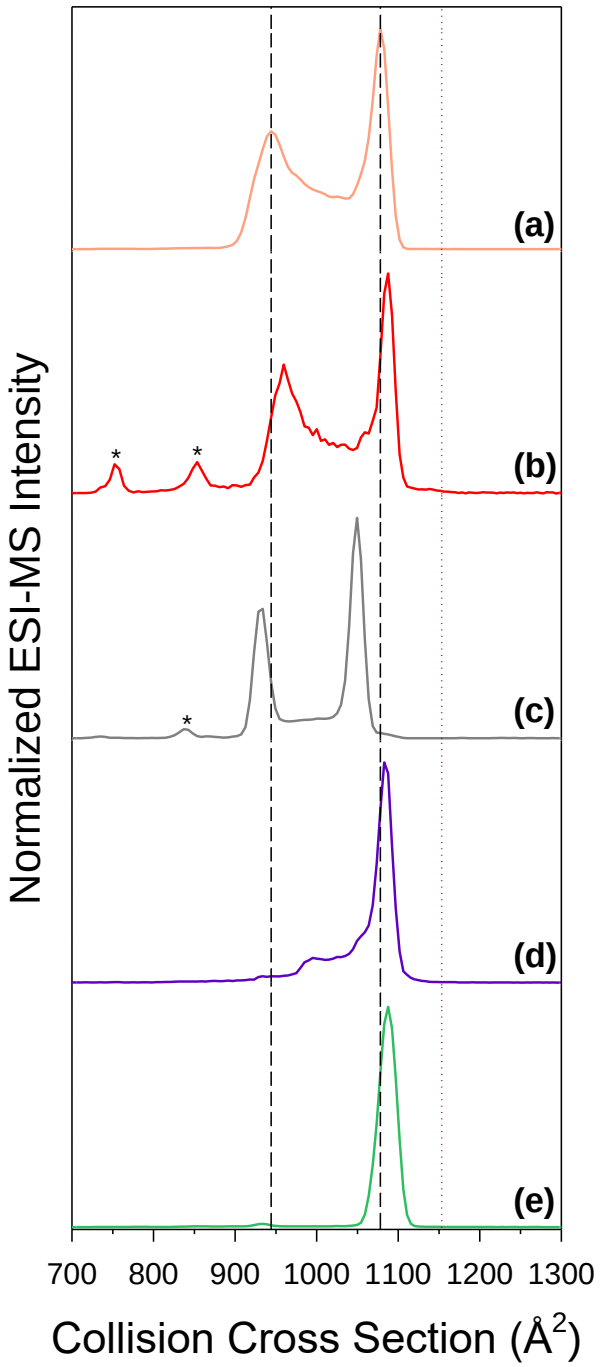

Figure 2. CCS distributions of the $[M+4H]^{4+}$ charge state of (a) native enfuvirtide, (b) SAH-gp41$_{(638-673)}$(C), (c) SAH-gp41$_{(638-673)}$(E), (d) SAH-gp41$_{(638-673)}$(B), and (e) SAH-gp41$_{(638-673)}$(D). Dashed vertical lines correspond to peak maxima from native Enf and are for feature comparison. Dotted vertical line represents the calculated CCS value for a fully-helical Enf peptide. Asterisks in B and C denote peaks resulting from singly-charged contaminant ions.

In addition to the single-stapled constructs described above, we measured multiple double-stapled Enf peptides with IM-MS. Double stapling has been shown to dramatically increase peptide proteolytic stability when compared to both native and single-stapled versions.[18, 28] The CCS distribution depicted in Figure S3b supports the observation that the SAH-gp41$_{(638-673)}$(E) staple more clearly defined the Enf conformational landscape into two species, while the addition of the SAH-gp41$_{(638-673)}$(C) staple had little effect. Conversely, the addition of the SAH-gp41$_{(638-673)}$(B) staple shifted the majority of the peptide to an extended conformation (Fig. S3c). Finally, the SAH-gp41$_{(638-673)}$(C,D) double-stapled construct resulted in a CCS profile (Fig. S3d) indistinguishable from that of the SAH-gp41$_{(638-673)}$(D) single staple, further demonstrating that SAH-gp41$_{(638-673)}$(D) is the most helix-inducing staple investigated here, while the SAH-gp41$_{(638-673)}$(C) staple does little to alter the Enf conformational distribution.

Staple Positioning Alters Enf Conformational Dynamics

The ion mobility results presented above suggest that gas-phase measurements can be used as a rapid screening tool for assessing the helical content of stapled peptides. We next sought to investigate whether the gas-phase results would correlate with solution phase analysis. HDX-MS is sensitive to backbone hydrogen bonding in secondary structural elements, such as α-helices, and can report on the conformational dynamics of multiple co-existing populations.[60-62] Different kinetic exchange regimes for protein segments have been previously discussed.[63-65] Briefly, exchange in the EX2 regime occurs when hydrogen bonds undergo opening/closing transitions much faster than the chemical H→D exchange rate. Conversely, EX1 kinetics are observed when several amide hydrogens participate in opening/closing events much more slowly than the rate of chemical exchange. EX2 kinetics manifest in an isotopic envelope that gradually increases in *m/z* with exchange time, whereas bimodal distributions are a hallmark of EX1 exchange. HDX has previously been utilized to investigate stapled peptides,[28] and for the sequences tested it was shown that deuterium uptake at the initial time point (10 s) correlated

well with protease stability, but not helicity. We sought to determine whether this correlation was also present in the Enf constructs used in this study.

Representative HDX spectra for the native Enf $[M+4H]^{4+}$ ion and those of the four singly-stapled constructs are shown in Figure 3, and the average temporal deuterium uptake for each construct is summarized in Figure 4. In agreement with the CD and IM data, native Enf is highly dynamic in solution and was consequently fully exchanged at the earliest labeling time point. Rapid deuteration was also observed previously for a synthetic peptide derived from the Enf-analogous region in feline immunodeficiency virus gp36.[66] The SAH-gp41$_{(638-673)}$(C), SAH-gp41$_{(638-673)}$(E), and SAH-gp41$_{(638-673)}$(B) constructs all exhibited small amounts of protection at early time points, but became fully labeled within 10 min. In the cases of SAH-gp41$_{(638-673)}$(C) and SAH-gp41$_{(638-673)}$(E), this may have been predicted from the IM traces (Fig. 2), however more protection would have been expected for the SAH-gp41$_{(638-673)}$(B) construct. While SAH-gp41$_{(638-673)}$(B) exhibited significant helicity by CD and a largely extended structure by IM, the HDX results highlighted that the peptide is quite dynamic in solution and the observed secondary structure is relatively unstable. The clear outlier in the HDX dataset is the SAH-gp41$_{(638-673)}$(D) construct. The staple imparted significant protection from exchange at all time points, with complete labeling not yet achieved even after 4 h, indicative of extensive backbone hydrogen bonding nucleated by the staple with the protective umbrella extending for more than 20 amino acids. These results support the assignment of the single peak in the SAH-gp41$_{(638-673)}$(D) CCS distribution as a helical conformation. Interestingly, while all other peptides exhibited EX2 exchange kinetics, SAH-gp41$_{(638-673)}$(D) labeling proceeded largely in the EX1 regime,[67] with an unfolding transition half-life of ~1 min as estimated by peak width analysis.[63] Additional bubble-plot analysis performed in HXExpress[48] revealed that the exchange profiles observed for SAH-gp41$_{(638-673)}$(D) resulted from large-scale helix-unfolding events rather than distinct peptide conformations in solution (Fig. S4). Interestingly, the SAH-gp41$_{(638-673)}$(C, D) construct exhibited exchange kinetics intermediate to the SAH-gp41$_{(638-673)}$(C) and SAH-gp41$_{(638-673)}$(D) constructs. While the EX1 kinetics were not as

obvious as in the SAH-gp41$_{(638\text{-}673)}$(D) construct, the temporal widening[63] of the isotopic envelope revealed their presence in the double-stapled peptide (Fig. S5). This indicated that while the SAH-gp41$_{(638\text{-}673)}$(C) staple does little to affect the conformational dynamics of native Enf, it can suppress the unfolding events measured for SAH-gp41$_{(638\text{-}673)}$(D), or at least increase the transition half-life beyond the timescale of the current experiments.

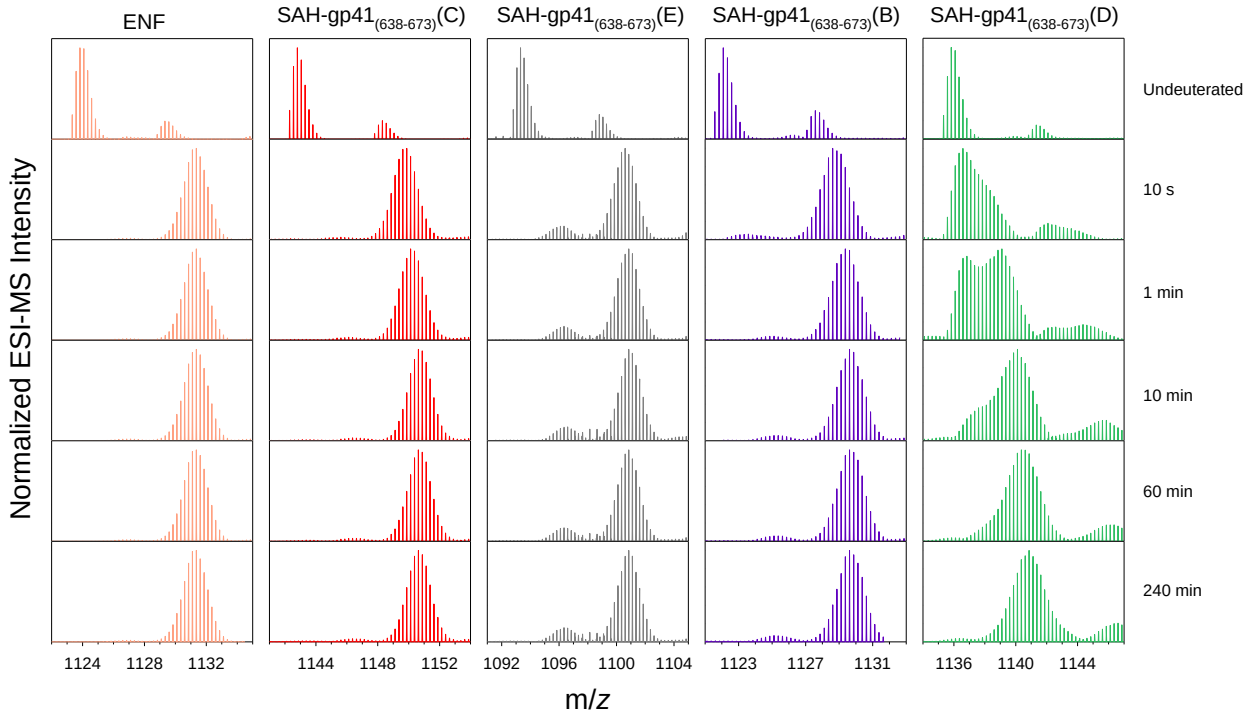

Figure 3. Hydrogen/deuterium exchange spectra of Enf and stapled constructs. Top spectrum of each column depicts the $[M+4H]^{4+}$ ion from the unlabeled sample and subsequent rows result from deuteration times ranging from 10 s to 4 h. Satellite isotopic envelopes in undeuterated spectra result from small amount of sodium adduction. Peptide color-coding mimics that of Figure 2 for clarity.

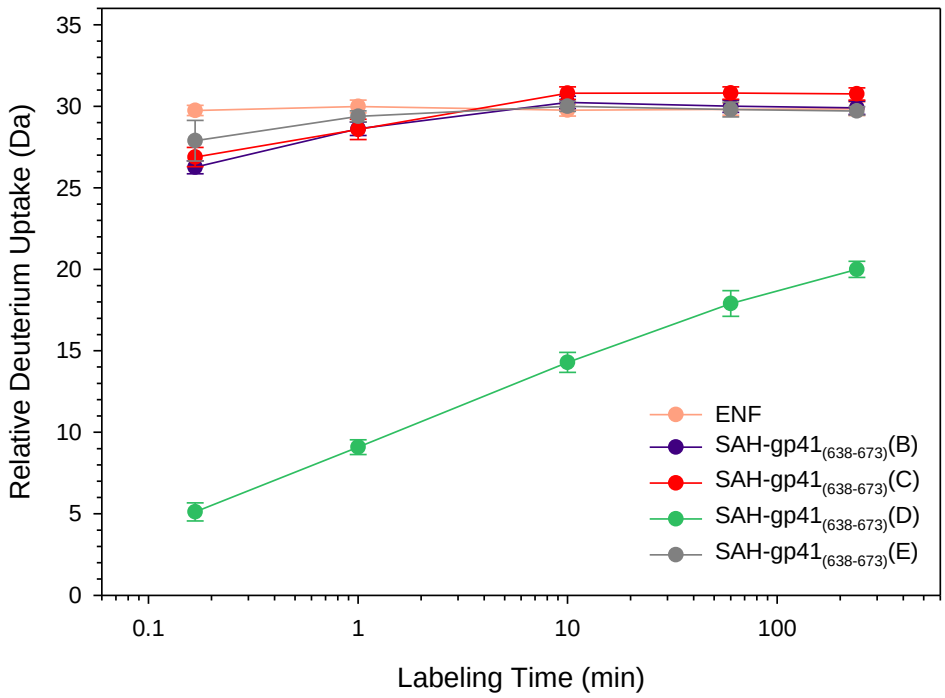

Figure 4. Deuterium uptake plot depicting conformational dynamics of native enfuvirtide (orange), and stapled constructs SAH-gp41$_{(638-673)}$(C) (red), SAH-gp41$_{(638-673)}$(E) (purple), SAH-gp41$_{(638-673)}$(B) (green), and SAH-gp41$_{(638-673)}$(D) (grey). Averages and standard deviations were calculated using multiple charge states (4+ and 3+) acquired in triplicate experiments.

Connections between MS Results and Helicity

In the previous sections we presented MS-based results of Enf conformation and dynamics, and now we discuss the observed relationships between CCS measurements, deuterium labeling, and α-helicity. Figure 5a shows that the average collision cross section of the Enf constructs reasonably correlated with helical content (R^2 ~ 0.78), however when the width of the CCS distribution was taken into account, the correlation improved dramatically (Fig. 5b). The width of the distribution speaks to the conformational landscape available to the peptide construct. A broad distribution, as in the case of native Enf (Fig. 2a), indicates conformational fluidity while a narrow peak (SAH-gp41$_{(638-673)}$(D), Fig. 2e) reflects a more defined structure.

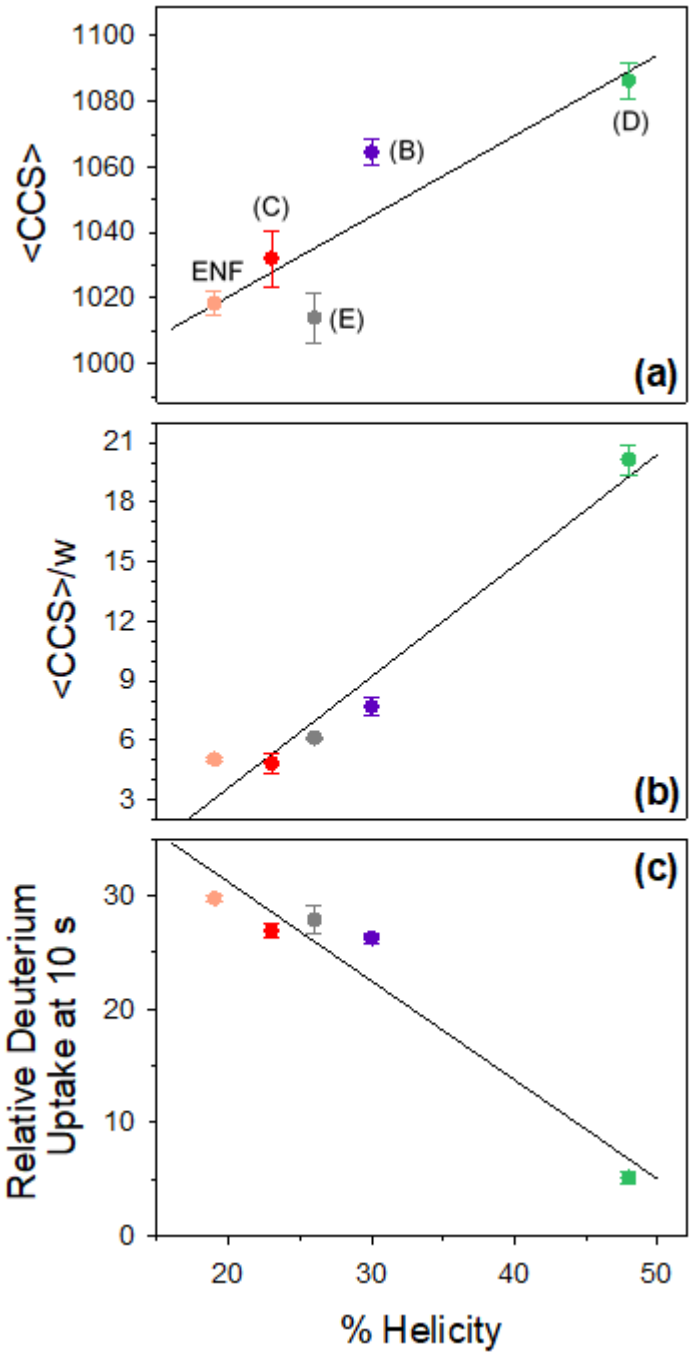

Figure 5. Correlation between mass spectrometry results and helical content. (a) Average collision cross section (R^2 ~ 0.78), (b) distribution width-corrected average CCS (R^2 ~ 0.95), and (c) relative deuterium uptake after 10 s of exchange (R^2 ~ 0.93), as a function of α-helicity measured by circular dichroism. Data points and error bars are averages and standard deviations, respectively, from triplicate measurements. Lettering in (a) corresponds to staple locations as described in Table 1.

While the IM data are acquired in the gas-phase, the CD measurements take place in solution. Thus it is interesting to compare the CD results with the solution-phase HDX dataset. The relative deuterium uptake at the earliest (10 s) time point for the Enf constructs exhibited very good correlation with α-helicity (Fig. 5c). This finding contrasts with results published by Shi *et al*. showing that deuterium uptake of stapled borealin peptides correlates with proteolytic stability rather than helicity.[28] Such differences conceivably derive from the distinct sequence compositions and lengths of peptides investigated, as well as the different proteases used and the corresponding number of potential cleavage sites. We note that for the constructs studied here, HDX reasonably correlates with proteolytic stability, provided the SAH-gp41$_{(638\text{-}673)}$(E) construct is removed from consideration (Fig. S6). Indeed, in the latter case, the E staple does not afford prominent α-helical stabilization (consistent with the HDX results) but does confer marked proteolytic stability due to the closer proximity of its C-terminal staple to sites of proteolytic vulnerability, namely the WNWF sequence. In a prior study of (*i, i+4*), (*i,i+3)* double-stapled membrane proximal external region (MPER) HIV-1 peptides,[68] the identical phenomenon was observed, with 6-fold enhancement in proteolytic stability simply by moving the same *i,i+4* staple two residues closer to the WNWF residues. In the context of the Enf peptide, which also includes this sequence, moving the D staple two residues downstream to the E staple position results in a 3-fold enhancement in chymotrypsin resistance. It is noteworthy that the E staple also replaces two Trp residues of the native sequence. Taken together, HDX provides a high precision read-out of stapling effects on peptide structure and proteolytic resistance, as recently demonstrated for hydrocarbon-stitched GLP1 peptides.[34] Our SAH-gp41$_{(638\text{-}673)}$(E) results highlight that when proteolytic resistance derives more from sequence-specific staple protection rather than α-helical induction, HDX naturally favors detection of the conformational rather than proteolytic changes. Thus, coupling the MS analyses to studying the resistance patterns to multiple proteases should

prove useful in distinguishing between the effect of hydrocarbon stapling on peptide conformation and localized protection of vulnerable sequences.

CONCLUSIONS

Hydrocarbon-stapled peptides often exhibit increased α-helicity and protease resistance in comparison to their native versions, and determining the optimal staple type and position is critical for maximizing biological activity. Here we demonstrated the utility of mass spectrometry in analyzing the conformation and dynamics of stapled peptides, both in solution and in the gas phase. Native enfuvirtide was determined to be highly dynamic by ion mobility and hydrogen exchange, consistent with previous experimental and computational studies. The C-terminally stapled SAH-gp41$_{(638\text{-}673)}$(D) construct exhibited the narrowest IM distribution with the largest average CCS value, indicative of a stabilized α-helical conformation. Solution-phase HDX measurements on a series of single-stapled Enf constructs revealed that a variety of staple positions had little effect on conformational dynamics when compared to the native peptide. However, one single-stapled construct in particular, SAH-gp41$_{(638\text{-}673)}$(D), was found to be highly protected from exchange, indicative of extensive hydrogen bonding of backbone amides, which again points to an induced α-helical conformation. The readouts of these MS experiments exhibited good correlation with average helical content measurements by circular dichroism, providing justification for their utility in the development and optimization of stapled peptides. These MS-based techniques require small sample amounts and the ability to differentiate numerous constructs by *m/z* should facilitate sample multiplexing to further decrease sample analysis times.

REFERENCES

(1) Henninot, A., Collins, J. C. and Nuss, J. M. The Current State of Peptide Drug Discovery: Back to the Future? *J. Med. Chem.* **2018**, *61*, 1382-1414.

(2) Fosgerau, K. and Hoffmann, T. Peptide therapeutics: current status and future directions. *Drug Discovery Today* **2015**, *20*, 122-128.

(3) Albericio, F. and Kruger, H. G. Therapeutic Peptides. *Future Med. Chem.* **2012**, *4*, 1527-1531.

(4) Vlieghe, P., Lisowski, V., Martinez, J. and Khrestchatisky, M. Synthetic Therapeutic Peptides: Science and Market. *Drug Discovery Today* **2010**, *15*, 40-56.

(5) Wu, D., Gao, Y., Qi, Y., Chen, L., Ma, Y. and Li, Y. Peptide-based Cancer Therapy: Opportunity and Challenge. *Cancer Lett.* **2014**, *351*, 13-22.

(6) Redman, J. S., Francis, J. N., Marquardt, R., Papac, D., Mueller, A. L., Eckert, D. M., Welch, B. D. and Kay, M. S. Pharmacokinetic and Chemical Synthesis Optimization of a Potent D-Peptide HIV Entry Inhibitor Suitable for Extended-Release Delivery. *Mol. Pharmaceutics* **2018**, *15*, 1169-1179.

(7) Cheng, S., Wang, Y., Zhang, Z., Lv, X., Gao, G. F., Shao, Y., Ma, L. and Li, X. Enfuvirtide-PEG Conjugate: A Potent HIV Fusion Inhibitor with Improved Pharmacokinetic Properties. *Eur. J. Med. Chem.* **2016**, *121*, 232-237.

(8) Cheng, S., Chang, X., Wang, Y., Gao, G. F., Shao, Y., Ma, L. and Li, X. Glycosylated Enfuvirtide: A Long-Lasting Glycopeptide with Potent Anti-HIV Activity. *J. Med. Chem.* **2015**, *58*, 1372-1379.

(9) Welch, B. D., VanDemark, A. P., Heroux, A., Hill, C. P. and Kay, M. S. Potent D-peptide inhibitors of HIV-1 entry. *Proc. Natl. Acad. Sci. U. S. A.* **2007**, *104*, 16828-33.

(10) Dwyer, J. J., Wilson, K. L., Davison, D. K., Freel, S. A., Seedorff, J. E., Wring, S. A., Tvermoes, N. A., Matthews, T. J., Greenberg, M. L. and Delmedico, M. K. Design of helical, oligomeric HIV-1 fusion inhibitor peptides with potent activity against enfuvirtide-resistant virus. *Proc. Natl. Acad. Sci. U. S. A.* **2007**, *104*, 12772-7.

(11) Bird, G. H., Bernal, F., Pitter, K. and Walensky, L. D. Synthesis and Biophysical Characterization of Stabilized α-Helices of BCL-2 Domains. *Methods Enzymol.* **2008**, *446*, 369-386.

(12) Walensky, L. D. and Bird, G. H. Hydrocarbon-stapled peptides: principles, practice, and progress. *J. Med. Chem.* **2014**, *57*, 6275-88.

(13) Cromm, P. M., Spiegel, J. and Grossmann, T. N. Hydrocarbon Stapled Peptides as Modulators of Biological Function. *ACS Chem. Biol.* **2015**, *10*, 1362-1375.

(14) Azzarito, V., Long, K., Murphy, N. S. and Wilson, A. J. Inhibition of α-helix-mediated protein-protein interactions using designed molecules. *Nat. Chem.* **2013**, *5*, 161-73.

(15) Pal, A., Neo, K., Rajamani, L., Ferrer, F. J., Lane, D. P., Verma, C. S. and Mortellaro, A. Inhibition of NLRP3 inflammasome activation by cell-permeable stapled peptides. *Sci. Rep.* **2019**, *9*, 4913.

(16) Bird, G. H., Boyapalle, S., Wong, T., Opoku-Nsiah, K., Bedi, R., Crannell, W. C., Perry, A. F., Nguyen, H., Sampayo, V., Devareddy, A., Mohapatra, S., Mohapatra, S. S. and Walensky, L. D. Mucosal delivery of a double-stapled RSV peptide prevents nasopulmonary infection. *J. Clin. Invest.* **2014**, *124*, 2113-24.

(17) Schafmeister, C. E., Po, J. and Verdine, G. L. An All-Hydrocarbon Cross-Linking System for Enhancing the Helicity and Metabolic Stability of Peptides. *J. Am. Chem. Soc.* **2000**, *122*, 5891-5892.

(18) Bird, G. H., Madani, N., Perry, A. F., Princiotto, A. M., Supko, J. G., He, X., Gavathiotis, E., Sodroski, J. G. and Walensky, L. D. Hydrocarbon Double-Stapling Remedies the Proteolytic Instability of a Lengthy Peptide Therapeutic. *Proc. Natl. Acad. Sci. U. S. A.* **2010**, *107*, 14093-14098.

(19) Guo, Z., Mohanty, U., Noehre, J., Sawyer, T. K., Sherman, W. and Krilov, G. Probing the α-helical structural stability of stapled p53 peptides: molecular dynamics simulations and analysis. *Chem. Biol. Drug Des.* **2010**, *75*, 348-59.

(20) Benesch, J. L. and Ruotolo, B. T. Mass spectrometry: come of age for structural and dynamical biology. *Curr. Opin. Struct. Biol.* **2011**, *21*, 641-649.

(21) Eschweiler, J. D., Kerr, R., Rabuck-Gibbons, J. and Ruotolo, B. T. Sizing Up Protein-Ligand Complexes: The Rise of Structural Mass Spectrometry Approaches in the Pharmaceutical Sciences. *Annu. Rev. Anal. Chem.* **2017**, *10*, 25-44.

(22) Kaltashov, I. A., Bobst, C. E., Pawlowski, J. and Wang, G. Mass Spectrometry-based Methods in Characterization of the Higher Order Structure of Protein Therapeutics. *J. Pharm. Biomed. Anal.*

(23) Houde, D., Berkowitz, S. A. and Engen, J. R. The utility of hydrogen/deuterium exchange mass spectrometry in biopharmaceutical comparability studies. *J. Pharm. Sci.* **2011**, *100*, 2071-86.

(24) Berkowitz, S. A., Engen, J. R., Mazzeo, J. R. and Jones, G. B. Analytical tools for characterizing biopharmaceuticals and the implications for biosimilars. *Nat. Rev. Drug Discov.* **2012**, *11*, 527-40.

(25) Deng, B., Lento, C. and Wilson, D. J. Hydrogen deuterium exchange mass spectrometry in biopharmaceutical discovery and development - A review. *Anal. Chim. Acta* **2016**, *940*, 8-20.

(26) Campuzano, I. D. and Lippens, J. L. Ion mobility in the pharmaceutical industry: an established biophysical technique or still niche? *Curr. Opin. Chem. Biol.* **2018**, *42*, 147-159.

(27) Rogstad, S., Faustino, A., Ruth, A., Keire, D., Boyne, M. and Park, J. A Retrospective Evaluation of the Use of Mass Spectrometry in FDA Biologics License Applications. *J. Am. Soc. Mass Spectrom.* **2017**, *28*, 786-794.

(28) Shi, X., Wales, T. E., Elkin, C., Kawahata, N., Engen, J. R. and Annis, D. A. Hydrogen Exchange-Mass Spectrometry Measures Stapled Peptide Conformational Dynamics and Predicts Pharmacokinetic Properties. *Anal. Chem.* **2013**, *85*, 11185-11188.
(29) Straus, R. N. and Jockusch, R. A. Hydrogen-Deuterium Exchange and Electron Capture Dissociation to Interrogate the Conformation of Gaseous Melittin Ions. *J. Am. Soc. Mass Spectrom.* **2019**, *30*, 864-875.
(30) Harvey, S. R., Porrini, M., Stachl, C., MacMillan, D., Zinzalla, G. and Barran, P. E. Small-molecule inhibition of c-MYC:MAX leucine zipper formation is revealed by ion mobility mass spectrometry. *J. Am. Chem. Soc.* **2012**, *134*, 19384-92.
(31) Pierson, N. A., Chen, L., Russell, D. H. and Clemmer, D. E. *Cis-Trans* Isomerizations of Proline Residues Are Key to Bradykinin Conformations. *J. Am. Chem. Soc.* **2013**, *135*, 3186-3192.
(32) Fuller, D. R., Glover, M. S., Pierson, N. A., Kim, D., Russell, D. H. and Clemmer, D. E. Cis-->Trans Isomerization of Pro(7) in Oxytocin Regulates Zn(2+) Binding. *J. Am. Soc. Mass Spectrom.* **2016**, *27*, 1376-1382.
(33) Massonnet, P., Haler, J. R. N., Upert, G., Degueldre, M., Morsa, D., Smargiasso, N., Mourier, G., Gilles, N., Quinton, L. and De Pauw, E. Ion Mobility-Mass Spectrometry as a Tool for the Structural Characterization of Peptides Bearing Intramolecular Disulfide Bond(s). *J. Am. Soc. Mass Spectrom.* **2016**, *27*, 1637-1646.
(34) Bird, G. H., Fu, A., Escudero, S., Godes, M., Opoku-Nsiah, K., Wales, T. E., Cameron, M. D., Engen, J. R., Danial, N. N. and Walensky, L. D. Hydrocarbon-Stitched Peptide Agonists of Glucagon-Like Peptide-1 Receptor. *ACS Chem. Biol.* **2020**, *15*, 1340-1348.
(35) LaBonte, J., Lebbos, J. and Kirkpatrick, P. Enfuvirtide. *Nat. Rev. Drug Discov.* **2003**, *2*, 345-6.
(36) Ashkenazi, A., Wexler-Cohen, Y. and Shai, Y. Multifaceted Action of Fuzeon as Virus-Cell Membrane Fusion Inhibitor. *Biochim. Biophys. Acta, Biomembr.* **2011**, *1808*, 2352-2358.
(37) Kilby, J. M., Hopkins, S., Venetta, T. M., DiMassimo, B., Cloud, G. A., Lee, J. Y., Alldredge, L., Hunter, E., Lambert, D., Bolognesi, D., Matthews, T., Johnson, M. R., Nowak, M. A., Shaw, G. M. and Saag, M. S. Potent Suppression of HIV-1 Replication in Humans by T-20, a Peptide Inhibitor of gp41-Mediated Virus Entry. *Nat. Med.* **1998**, *4*, 1302-1307.
(38) Biron, Z., Khare, S., Quadt, S. R., Hayek, Y., Naider, F. and Anglister, J. The 2F5 Epitope is Helical in the HIV-1 Entry Inhibitor T-20. *Biochemistry* **2005**, *44*, 13602-13611.
(39) Singh, P., Sharma, P., Bisetty, K., Corcho, F. J. and Perez, J. J. Comparative structural studies of T-20 analogues using molecular dynamics. *Comput. Theor. Chem.* **2011**, *974*, 122-132.
(40) Joyce, J. G., Hurni, W. M., Bogusky, M. J., Garsky, V. M., Liang, X., Citron, M. P., Danzeisen, R. C., Miller, M. D., Shiver, J. W. and Keller, P. M. Enhancement of α-helicity in the HIV-1 inhibitory peptide DP178 leads to an increased affinity for human monoclonal antibody 2F5 but does not elicit neutralizing responses *in vitro*. *J. Biol. Chem.* **2002**, *277*, 45811-20.
(41) Bird, G. H., Mazzola, E., Opoku-Nsiah, K., Lammert, M. A., Godes, M., Neuberg, D. S. and Walensky, L. D. Biophysical determinants for cellular uptake of hydrocarbon-stapled peptide helices. *Nat. Chem. Biol.* **2016**, *12*, 845-52.
(42) Stocks, B. B. and Melanson, J. E. In-Source Reduction of Disulfide-Bonded Peptides Monitored by Ion Mobility Mass Spectrometry. *J. Am. Soc. Mass Spectrom.* **2018**, *29*, 742-751.
(43) Bush, M. F., Campuzano, I. D. G. and Robinson, C. V. Ion Mobility Mass Spectrometry of Peptide Ions: Effects of Drift Gas and Calibration Strategies. *Anal. Chem.* **2012**, *84*, 7124-7130.
(44) Vahidi, S., Stocks, B. B. and Konermann, L. Partially Disordered Proteins Studied by Ion Mobility-Mass Spectrometry: Implications for the Preservation of Solution Phase Structure in the Gas Phase. *Anal. Chem.* **2013**, *85*, 10471-10478.
(45) Buzon, V., Natrajan, G., Schibli, D., Campelo, F., Kozlov, M. M. and Weissenhorn, W. Crystal structure of HIV-1 gp41 including both fusion peptide and membrane proximal external regions. *PLoS Pathog.* **2010**, *6*, e1000880.
(46) Ewing, S. A., Donor, M. T., Wilson, J. W. and Prell, J. S. Collidoscope: An Improved Tool for Computing Collisional Cross-Sections with the Trajectory Method. *J. Am. Soc. Mass Spectrom.* **2017**, *28*, 587-596.
(47) Weis, D. D., Engen, J. R. and Kass, I. J. Semi-automated data processing of hydrogen exchange mass spectra using HX-Express. *J. Am. Soc. Mass Spectrom.* **2006**, *17*, 1700-3.
(48) Guttman, M., Weis, D. D., Engen, J. R. and Lee, K. K. Analysis of overlapped and noisy hydrogen/deuterium exchange mass spectra. *J. Am. Soc. Mass Spectrom.* **2013**, *24*, 1906-12.
(49) Wales, T. E. and Engen, J. R. Hydrogen exchange mass spectrometry for the analysis of protein dynamics. *Mass Spectrom Rev* **2006**, *25*, 158-70.
(50) Judice, J. K., Tom, J. Y. K., Huang, W., Wrin, T., Vennari, J., Petropoulos, C. J. and McDowell, R. S. Inhibition of HIV type 1 infectivity by constrained a-helical peptides: Implications for the viral fusion mechanism. *Proc. Natl. Acad. Sci. U. S. A.* **1997**, *94*, 13426-13430.
(51) Chang, D., Kolis, S. J., Linderholm, K. H., Julian, T. F., Nachi, R., Dzerk, A. M., Lin, P. P., Lee, J. W. and Bansal, S. K. Bioanalytical method development and validation for a large peptide HIV fusion inhibitor (Enfuvirtide, T-20) and its metabolite in human plasma using LC-MS/MS. *J. Pharm. Biomed. Anal.* **2005**, *38*, 487-96.
(52) Bakhtiari, M. and Konermann, L. Protein Ions Generated by Native Electrospray Ionization: Comparison of Gas Phase, Solution, and Crystal Structures. *J. Phys. Chem. B* **2019**, *123*, 1784-1796.

(53) Sivalingam, G. N., Cryar, A., Williams, M. A., Gooptu, B. and Thalassinos, K. Deconvolution of ion mobility mass spectrometry arrival time distributions using a genetic algorithm approach: Application to α1-antitrypsin peptide binding. *Int. J. Mass Spectrom.* **2018**, *426*, 29-37.
(54) Kaleta, D. T. and Jarrold, M. F. Helix-turn-helix motifs in unsolvated peptides. *J. Am. Chem. Soc.* **2003**, *125*, 7186-7.
(55) Kohtani, M., Jones, T. C., Schneider, J. E. and Jarrold, M. F. Extreme Stability of an Unsolvated α-Helix. *J. Am. Chem. Soc.* **2004**, *126*, 7420-7421.
(56) Jarrold, M. F. Helices and Sheets in vacuo. *Phys. Chem. Chem. Phys.* **2007**, *9*, 1659-71.
(57) Morrison, L. J. and Wysocki, V. H. Gas-phase helical peptides mimic solution-phase behavior. *J. Am. Chem. Soc.* **2014**, *136*, 14173-83.
(58) Sallam, S., Dolog, I., Paik, B. A., Jia, X., Kiick, K. L. and Wesdemiotis, C. Sequence and Conformational Analysis of Peptide-Polymer Bioconjugates by Multidimensional Mass Spectrometry. *Biomacromolecules* **2018**, *19*, 1498-1507.
(59) Martins Do Canto, A. M., Palace Carvalho, A. J., Prates Ramalho, J. P. and Loura, L. M. S. T-20 and T-1249 HIV fusion inhibitors' structure and conformation in solution: a molecular dynamics study. *J. Pept. Sci.* **2008**, *14*, 442-7.
(60) Konermann, L., Tong, X. and Pan, Y. Protein structure and dynamics studied by mass spectrometry: H/D exchange, hydroxyl radical labeling, and related approaches. *J Mass Spectrom* **2008**, *43*, 1021-36.
(61) Engen, J. R. Analysis of Protein Conformation and Dynamics by Hydrogen/Deuterium Exchange MS. *Anal. Chem.* **2009**, *81*, 7870-7875.
(62) Zheng, J., Strutzenberg, T., Pascal, B. D. and Griffin, P. R. Protein dynamics and conformational changes explored by hydrogen/deuterium exchange mass spectrometry. *Curr. Opin. Struct. Biol.* **2019**,
(63) Weis, D. D., Wales, T. E., Engen, J. R., Hotchko, M. and Ten Eyck, L. F. Identification and characterization of EX1 kinetics in H/D exchange mass spectrometry by peak width analysis. *J. Am. Soc. Mass Spectrom.* **2006**, *17*, 1498-1509.
(64) Konermann, L., Pan, J. and Liu, Y. H. Hydrogen exchange mass spectrometry for studying protein structure and dynamics. *Chem Soc Rev* **2011**, *40*, 1224-34.
(65) Nielsen, A. K., Moller, I. R., Wang, Y., Rasmussen, S. G. F., Lindorff-Larsen, K., Rand, K. D. and Loland, C. J. Substrate-induced conformational dynamics of the dopamine transporter. *Nat. Commun.* **2019**, *10*, 2714.
(66) Desmaris, F., Lemaire, D., Ricard-Blum, S., Chatrenet, B. and Forest, E. Structural characterization of the feline-immunodeficiency-virus envelope glycoprotein 36 ectodomain for the development of new antivirals. *Biochem. J.* **2005**, *389*, 559-567.
(67) Krishna, M. M., Hoang, L., Lin, Y. and Englander, S. W. Hydrogen exchange methods to study protein folding. *Methods* **2004**, *34*, 51-64.
(68) Bird, G. H., Irimia, A., Ofek, G., Kwong, P. D., Wilson, I. A. and Walensky, L. D. Stapled HIV-1 peptides recapitulate antigenic structures and engage broadly neutralizing antibodies. *Nat. Struct. Mol. Biol.* **2014**, *21*, 1058-67.